

## Sub-10 nm Thick Microporous Membranes Made by Plasma-Defined Atomic Layer Deposition of a Bridged Silsesquioxane Precursor

Ying-Bing Jiang,<sup>†</sup> George Xomeritakis,<sup>‡</sup> Zhu Chen,<sup>‡</sup> Darren Dunphy,<sup>‡</sup> David J. Kissel,<sup>‡</sup>  
Joseph L. Cecchi,<sup>\*,‡</sup> and C. Jeffrey Brinker<sup>\*,†,‡</sup>

Sandia National Laboratories, Department 1815, MS 1349, PO Box 5800, Albuquerque, New Mexico 87185, and  
Department of Chemical and Nuclear Engineering, University of New Mexico, Albuquerque, New Mexico 87131

Received September 24, 2007; E-mail: cjbrink@sandia.gov; cecchi@unm.edu

Membranes exhibiting high flux and selectivity are important for many applications, including water desalination, greenhouse gas storage and abatement, H<sub>2</sub> purification, and selective proton/oxygen conduction in fuel cells. Combined high flux and selectivity is achieved in natural systems by membrane-bound ion and molecular channels—whose pore size is defined with sub-nanometer precision through protein folding and whose thickness is limited to that of the cellular membrane bilayer, only 4 nm. By comparison, synthetic membranes can seldom be fabricated with similar molecular level precision (the exceptions being carbon nanotubes and zeolites) and are often 100–1000× thicker. This is problematic because membrane flux varies reciprocally with membrane thickness. The inherent issue is that most synthetic approaches require relatively thick membranes to avoid defects or, in the case of zeolites and CNTs, the smallest-sized building blocks used for membrane fabrication are of the order 1  $\mu\text{m}$ .<sup>1,2</sup>

Here we describe an atomic layer deposition (ALD) approach to construct ultrathin membranes with sub-angstrom control of pore size. Our approach extends the burgeoning ALD field<sup>3–7</sup> in several new directions. First, we perform ALD on a self-assembled nanoporous support, where the internal porosity is protected from deposition. Second, we restrict ALD to the extreme surface by plasma activation. Third, we employ a bridged bis-silsesquioxane precursor to deposit a hybrid organosilicate film, uniformly incorporating organic ligands that serve as molecular templates/porogens upon subsequent removal. Beyond membrane formation, this plasma-directed ALD approach naturally forms a low *k* dielectric sealing layer needed for future generations of microelectronics.

ALD is a self-limiting layer-by-layer thin film deposition technique composed normally of successive steps of adsorption and hydrolysis/activation of metal halide or metal alkoxide precursors.<sup>3–6</sup> To date, ALD has focused principally on the formation of dense thin film oxides, metals, or semiconductor alloys on solid substrates. Our previous research introduced plasma-assisted (PA)-ALD as a means to deposit dense oxide films on the immediate surface of a nanoporous film. In PA-ALD, exposure to a remote Ar + O<sub>2</sub> plasma, rather than hydrolysis, is used to activate the surface through formation of hydroxyl groups. Because both the plasma Debye length and the radical mean free path exceed greatly the pore diameter (~3 nm; see Figure 1), deposition does not occur within the interior pores.<sup>7</sup>

Surface-limited deposition of ultrathin layers on porous supports is important for sealing low *k* dielectrics. It is also of interest in the formation of high flux membranes. Here we achieve surface-limited deposition and develop a high flux, high selectivity membrane by an approach combining remote plasma exposure and surface passivation with conventional ALD of an (unconventional)

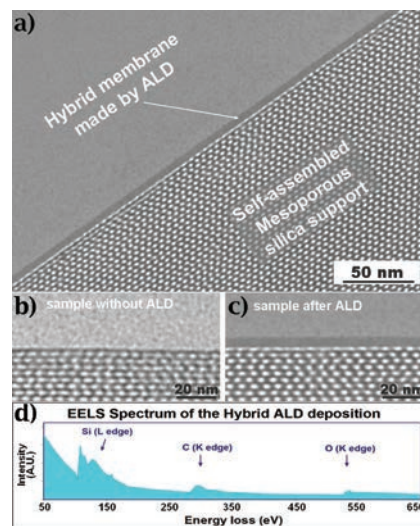


**Figure 1.** (a) Cross-sectional TEM image of the hybrid membrane supported on mesoporous silica; (b) original mesoporous silica support; (c) support coated with ALD membrane; (d) EELS spectrum of the membrane.

hybrid precursor (see also Supporting Information). We start with a nanoporous silica film (Figure 1), consisting of an ordered cubic arrangement of monosized pores, formed by evaporation-induced self-assembly<sup>8</sup> on an underlying anodized alumina support having 20 nm pores aligned normal to the support surface. Following calcination and UV/ozone exposure,<sup>9</sup> the nanoporous film has fully hydroxylated 3.2 nm pores as measured by a surface acoustic wave based technique.<sup>10</sup> To avoid ALD on any interior porosity, which would detrimentally increase the membrane thickness, we expose this hierarchical membrane support structure to hexamethyldisilazane and then to trimethylchlorosilane vapor at 180 °C for 5 min. This exposure converts the surface and internal hydroxyl groups to trimethylsiloxane groups, which remain inert to hydrolysis reactions and therefore passivate the surface against ALD during subsequent steps. To activate the immediate surface of the nanoporous film to ALD, the sample is exposed to a remote Ar + O<sub>2</sub> plasma for 2 s. As reported previously by us, the plasma was designed so that its Debye length (several mm) and radical mean free path (several mm) are much larger than the pore size.<sup>7</sup> In this condition, the plasma radicals cannot penetrate the internal porosity, and only trimethylsiloxane groups residing on the immediate surface of the nanoporous film are converted to silanols  $\equiv\text{Si}-\text{OH}$ . These surface silanols are active to halide and alkoxide ALD precursors,  $\text{M}(\text{X})_n$  and  $\text{M}(\text{OR})_n$ , respectively, undergoing condensation reactions to form  $\equiv\text{Si}-\text{O}-\text{M}\equiv$  plus HX and HOR byproducts. Therefore, ALD takes place on the surface of the substrate, while internal, hydrophobic  $-\text{Si}(\text{CH}_3)_3$  groups remain unhydrolyzed and do not undergo condensation reactions with ALD precursors.

<sup>†</sup> Sandia National Laboratories.

<sup>‡</sup> University of New Mexico.

In the case of passivated internal porosity, successive steps of adsorption and hydrolysis of  $M(X)_n$  and  $M(OR)_n$  precursors first reduce the size of surface nanopores and then, when the film thickness exceeds the original pore radius, progressively seal the surface. If molecular-sized pore templates, so-called porogens, could be introduced within a dense, ultrathin sealing layer, their removal would create a corresponding ultrathin microporous membrane with controlled pore size and shape.<sup>11–13</sup> Introduction of organic templates using organosilanes  $R_xSiX_{4-x}$  is rather straightforward and has been demonstrated previously.<sup>5,12</sup> However, in this case, the condensation reactions position the organic ligands  $R$  on the external surface, where they passivate it toward further ALD. Additionally, the coverage of  $R$  groups must be sufficiently low so as to avoid association of multiple  $R$  groups, which when removed would create larger and more polydisperse pores than individual  $R$  groups. To resolve these problems, we used an organically bridged silsesquioxane  $(RO)_3Si-R'-Si(OR)_3$  as an ALD precursor. In this case, the  $R'$  unit, which serves as the pore template, is incorporated uniformly within the developing siloxane framework, avoiding passivation of the surface and reducing template aggregation.

Here, as an example, we describe ALD of BTEE (bis(triethoxysilyl)ethane,  $(C_2H_5O)_3Si-C_2H_4-Si(OC_2H_5)_3$ ). Following remote plasma exposure to activate the nanoporous substrate, ALD was performed in a home-built reactor according to the following steps: (1) evacuate ALD chamber to a base vacuum of  $10^{-6}$  Torr; (2) inject BTEE vapor, causing BTEE molecules to condense with surface  $\equiv Si-OH$  groups; (3) purge chamber with Ar to remove all non-condensed BTEE and condensation byproducts; (4) inject water vapor to hydrolyze the ethoxysilane groups of surface chemisorbed BTEE; (5) purge chamber with Ar to remove residual water vapor and ethanol byproducts; (6) repeat steps 2–5 to obtain desired thickness.

Figure 1a shows a representative cross-sectional TEM image of the nanoporous supported ALD film prepared by 300 cycles of ALD (each cycle comprising steps 2–5 above) followed by UV/ozone exposure to remove the organic  $C_2$  template. The film is ultrathin ( $\sim 5$  nm thick) and smooth and spans the  $\sim 3$  nm diameter pores of the underlying support. The somewhat lower electron contrast with respect to silica derives from its sub-nanometer microporosity (see following discussion) not resolvable in this image. Comparison of the higher magnification images in Figure 1b (support prior to ALD) and Figure 1c (support after ALD) shows that the film is confined to the immediate surface of the support with no evidence of penetration into the nanoporous sublayer. Figure 1d shows the electron energy loss spectrum (EELS) of the as-deposited ALD film. Prior to EELS, the sample was cleaned in a plasma oxidizer to remove any carbon contamination on the sample surface as well as epoxy used for cross-sectional sample preparation. The energy loss edges at 104, 286, and 540 eV are attributed to Si, C, and O, respectively. The absence of a shoulder edge at  $\sim 282$  eV indicates that the carbon is mainly  $\sigma$ -bonded as expected from the bridging ethylene group in the BTEE precursor.<sup>14</sup>

To demonstrate the efficacy of this approach to form selective membranes, the organic template was removed by 30 s of UV/ozone exposure, and the permeance of the film to the series of gases He,  $N_2$ , and  $SF_6$  was measured at room temperature using standard techniques.<sup>11,12</sup> Figure 2 shows the gas permeances and selectivities of the samples after differing numbers of ALD cycles. The original porous support had a He permeance of  $171 \text{ cm}^3/\text{bar}\cdot\text{cm}^2\cdot\text{min}$  and He/ $N_2$  selectivity and He/ $SF_6$  selectivity of 2.08 and 4.28, consistent with Knudsen diffusion. With increasing cycle numbers, the permeance decreased, and after 100 cycles, the selectivity increased

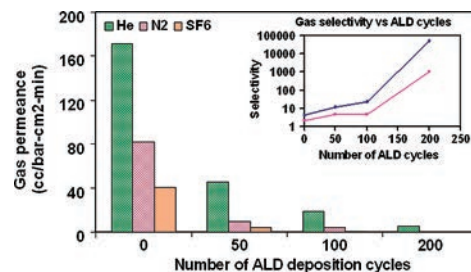


**Figure 2.** Gas permeances of ALD membranes to He,  $N_2$ , and  $SF_6$  with kinetic diameters of 2.2, 3.6, and 5.5 Å, respectively.

logarithmically. These results are consistent with the requirement to form a defect-free, pore-spanning sealing layer of several nanometer thickness prior to template removal. Due to the thinness of the membrane, after 200 ALD cycles, the He permeance was a very remarkable  $5.3 \text{ cm}^3/\text{bar}\cdot\text{cm}^2\cdot\text{min}$ , and the He/ $N_2$  and He/ $SF_6$  selectivities exceeded  $10^3$  and  $10^4$ , respectively.

In order to demonstrate the importance of bridging, rather than pendant, organic templates to this membrane fabrication strategy, we attempted to perform ALD using organosilane precursors, such as  $R'-SiX_3$ ,  $R'-Si(OR)_3$ , and  $(R'-SiX_2)_2O$ , but we found the deposition rate to be practically zero, presumably due to surface passivation.

We have established a route to fabricate ultrathin hybrid organic/inorganic sealing layers on porous supports and to convert them to high flux/selectivity membranes by removal of the bridging organic template. Prior to conversion, these materials are of interest for low  $k$  sealing layers. Use of  $R'$  ligands with other shapes and sizes should enable this route to be generalized to many different demanding separation problems. Through intermittent replacement of BTEE with  $TiCl_4$  or  $ZrCl_4$ , we expect to be able to increase further the thermal stability, allowing operation at higher temperatures.

**Acknowledgment.** This work was supported by DOE BES and NETL programs, the Army Research Office, Air Force Office of Scientific Research, the NIH Nanomedicine Center program, and the SNL LDRD program.

**Supporting Information Available:** Additional supporting figures are available. This material is available free of charge via the Internet at <http://pubs.acs.org>.

## References

- (1) Lai, Z.; Bonilla, G.; Diaz, I.; Nery, J.; Sujaoti, K.; Amat, M.; Kokkoli, E.; Thompson, R.; Tsapatsis, M.; Vlachos, D. *Science* **2003**, *300*, 456–460.
- (2) Holt, J.; Park, H.; Wang, Y.; Stadermann, M.; Artyukhin, A.; Grigoropoulos, C.; Noy, A.; Bakajin, O. *Science* **2006**, *312*, 1034–1037.
- (3) Cameron, M.; Gartland, I.; Smith, J.; Diaz, S.; George, S. M. *Langmuir* **2000**, *16*, 7435–7444.
- (4) Lim, B. S.; Rahtu, A.; Gordon, R. G. *Nat. Mater.* **2003**, *2*, 749–754.
- (5) Ek, S.; Iiskola, E. I.; Niinistö, L. *Langmuir* **2003**, *19*, 3461–3471.
- (6) Chen, R.; Bent, S. F. *Adv. Mater.* **2006**, *18*, 1086.
- (7) Jiang, Y. B.; Liu, N. G.; Gerung, H.; Cecchi, J. L.; Brinker, C. J. *J. Am. Chem. Soc.* **2006**, *128*, 11018–11019.
- (8) Brinker, C. J.; Lu, Y. F.; Sellinger, A.; Fan, H. Y. *Adv. Mater.* **1999**, *11*, 579–585.
- (9) Clark, T.; Ruiz, J.; Fan, H.; Brinker, C. J.; Swanson, B.; Parikh, A. *Chem. Mater.* **2000**, *12*, 3879–3884.
- (10) Hietala, S.; Hietala, V.; Brinker, C. J. *IEEE Transactions on Ultrasonics, Ferroelectrics, and Frequency Control* **2001**, *48*, 262–267.
- (11) Brinker, C. J.; Sehál, R.; Hietala, S.; Deshpande, R.; Smith, D.; Loy, D.; Ashley, C. S. *J. Membr. Sci.* **1994**, *94*, 85–102.
- (12) Raman, N.; Brinker, C. J. *J. Membr. Sci.* **1995**, *105*, 273–279.
- (13) Lu, Y.; Fan, H.; Doke, N.; Loy, D.; Assink, R.; LaVan, D.; Brinker, C. J. *J. Am. Chem. Soc.* **2000**, *122*, 5258–5261.
- (14) Schmid, H. K. *Microsc. Microanal. Microstruct.* **1995**, *6*, 99–111.